Journal of the Iranian Chemical Society (2023) 20:1405–1415
https://doi.org/10.1007/s13738-023-02765-2

ORIGINAL PAPER

Kinetic and computational study of the oxidative degradation of an amebicide by acid bromate in perchlorate solutions and the effect of Ruthenium (III) catalyst in micro molar concentration: a mechanistic approach

Naghmi Nigar Siddiqui[1] · Yougesh Dubey[1] · Amrita Srivastava[1]

Received: 13 September 2022 / Accepted: 30 January 2023 / Published online: 9 March 2023

Abstract
The oxidation of Metronidazole (MTZ) by potassium bromate was studied iodometrically in the acidic medium under pseudo-first-order conditions catalyzed by Ruthenium (III) between 303 K and 318 K. The stoichiometry of the reaction was found to be 1:1 and the rate law can be represented as $-d[BrO_3^-]/dt = [BrO_3^-][H^+]$. The rate of reaction was enormously intensified by the addition of Ru(III) catalyst in the concentration range 8.0×10^{-5}–8.0×10^{-4} mol dm^{-3}, confirmed by the linearity of the plot log k_c versus log[Ru(III)]($r \geq 0.9772$, $S \leq 0.04544$), while it was independent of the concentration of MTZ in the range 0.5×10^{-3} to 1.75×10^{-3} mol dm^{-3}. The main oxidation product identified was 2- (2-methyl-5-nitroimidazol-1-yl) acetaldehyde which was affirmed by IR absorption peaks at 1700-1720 cm^{-1} for aldehydic carbonyl group. UV–vis analysis of the product was also recorded. All quantum chemical calculations were performed by Density Functional Theory (DFT) with B3LYP/6-31G (d,p) basis atomic set for absolving the structure, reaction, and mechanism. Molecular orbital energies, bond length, bond angles, nonlinear optical properties, reactivity, and electrophilic and nucleophilic regions were emanated. The impact of various reactants on the rate of chemical reaction was also unearthed. A pertinent mechanism congruous with discerned kinetic results has been tendered, after which rate law emanated.

Keywords Oxidative degradation · Computational · Ruthenium (III) · Metronidazole · Potassium bromate

Introduction

Imidazoles have potent biological activities in humans like anti-inflammatory, antimycotic, antitumor, antiviral, antituberculotic, antimicrobial properties, etc. [1]. Metronidazole (MTZ) is a very prominent antiprotozoal drug to treat amoebiasis caused by a protozoan Entamoeba histolytica [2]. Structurally MTZ contains an electronegative nitro group attached in the imidazole moiety, which is the reducible center of the molecule [3].

✉ Amrita Srivastava
amrita.sri18@gmail.com

Naghmi Nigar Siddiqui
naghminigar@gmail.com

Yougesh Dubey
yougeshdubey74@gmail.com

[1] Department of Chemistry, University of Lucknow, Lucknow, Uttar Pradesh 226007, India

Bromate, Br (V), is known to be a powerful oxidizing agent with redox potentials of 1.44V in acidic medium and 0.61V in alkaline medium. The potentials show that bromine in basic solutions can be disproportionate simultaneously [4].

In recent times, the N-halosuccinimide have shown promising results in the system where it is exploited as positive halogen source. Although various reactions involving Br (V) as an oxidizing agent are known, still mechanistic and kinetic aspects of these reactions have yet received very little attention [4, 5]. To study these types in reaction detail, catalysis also plays an important role [6]. For this, Ruthenium (III) has been chosen as it shows a significant role in explaining redox reactions in detail [7].

Although oxidation–reduction reactions incorporating such catalyst and oxidant combinations reactions have been studied in detail, scant attention has been paid in using Potassium bromate as an oxidant in various metal-catalyzed reactions [6–11].

Molecular orbital calculations are widely used in the material, chemical and biological applications. These calculations elaborate the properties such as- (i) electronic coupling between the donor and acceptor species, (ii) structure and geometry, and (iii) nonlinear optical properties by hyper-polarizability calculations. The DFT calculations incorporate MESP, NLO, electronic absorption spectra, Global reactivity descriptors and thermodynamic properties were investigated using the DFT method with B3LYP function using 6-31G (d,p) basis atomic set. Global reactivity descriptors like electron affinity, electronegativity, ionization potential, electrophilicity index and chemical potential have been computed to anticipate the molecule's reactivity. These calculations also help to explain experimental data.

Literature Review reveals, it was found that no satisfactory information is available on the catalyzed oxidation kinetics of MTZ with any oxidant. There was a need to understand the oxidation mechanism of this drug in acidic and alkaline media that corresponds to the computational data as well. Santana et al. [12] reported that MTZ is a potential human carcinogen, as listed by International Agency for Research on Cancer, due to its genotoxic nature, mutagenicity and adverse influence on human DNA along with high solubility and low biodegrability. The study in this particular article was carried out to pave the way for future scope of MTZ and its oxidative product that can minimize aforesaid adverse effects of parent compound.

This compelled us to perform the present investigation, which includes Ru (III) catalyzed oxidation of MTZ by potassium bromate in an acidic medium so that its study could shed light on the drug's fate in the biological systems [13].

Experimental

Material and kinetic measurements

All the chemicals were A.R. grade and their respective solutions were prepared in the double distilled water [5]. A solution of MTZ (CDH Ltd, New Delhi) of required strength was prepared freshly [3]. The Stock solution of potassium bromate was prepared in double distilled water and its concentration was regularly checked iodometrically [14]. The stock solution of Ruthenium Chloride was prepared by dissolving the known amount in HCl of known strength in a darkened flask to avoid photochemical effects [15]. KCl, $HClO_4$, Hg $(OAc)_2$ of known strength were also used without further purification. Solutions used were freshly prepared for each kinetic run [5]. All the vessels used in the reaction were also coated black to dodge any photochemical reaction [16]. Aliquots of the reaction mixture were placed in the thermostat-controlled water bath, which was equilibrated at 313 K. Requisite volume of thermostatic MTZ solution was quickly pipetted out and then spewed into the reaction vessel. The total volume of the reaction mixture was 50 ml. 5 ml from the reaction mixture was sucked out at different intervals of time which was quenched with acidified potassium iodide solution. The advancement of the reaction was surveilled by iodometric estimation of oxidant unreacted in measured aliquots of the reaction mixture withdrawn at regular intervals. The kinetic runs were carried out at four different temperatures.

Computational details

Molecular orbital calculations of reactants and products for theoretical and experimental corroboration were done by density functional theory (DFT) with B3LYP [17] with 6-31G(d,p) as basis set with the Gaussian 09 package [18]. The graphical presentations of calculated IR and UV spectra were done by GaussView 06 program. At DFT/B3LYP level the NBO calculations [18] for complete geometrical optimization were carried out so as to interpret assorted second-order interactions. The time dependent density functional theory (TD-DFT) at B3LYP/6–31-G(d,p) level in solvent (Water) by using IEFPCM model was interpreted the frontier orbital analysis.

Results and discussion

Product identification and stoichiometry -

Varying ratios of $KBrO_3$ and MTZ reaction mixtures containing in the presence of $HClO_4$ at 303 K were kept aside for 48 h, so that the substrates can wholly convert into products [1]. Estimation of the unreacted $KBrO_3$ showed that one mole of substrate depleted one mole of oxidant in both cases [19]. The observed stoichiometry (1:1) for MTZ can be embodied by Scheme. The reaction product was of MTZ was found to be 2-(2-methyl-5-nitro-1H-imidazol-1-yl) acetaldehyde and extracted with ether and recrystallized from aqueous alcohol. The obtained product was detected by the 2,4-DNP derivative and conventional spot tests [20]. Further, the presence of aldehyde was confirmed by its IR absorption bands at 1700–1720 cm^{-1} for C = O stretching and at 2852 cm^{-1} for aldehydic C-H stretching modes (Fig. 1). The FT-IR

Scheme showing chemical reaction and stoichiometry of oxidation of MTZ by acidic potassium bromate

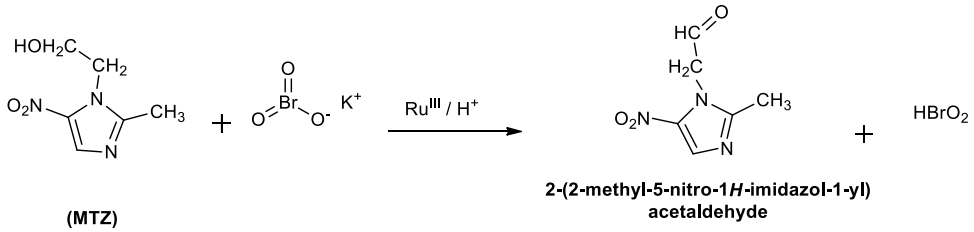

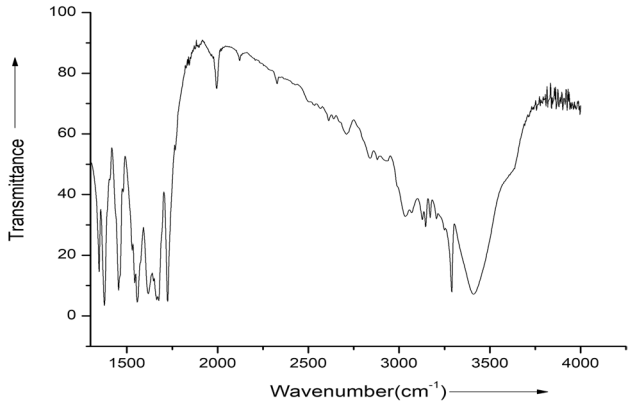

Fig. 1 FT-IR Spectra of reaction product

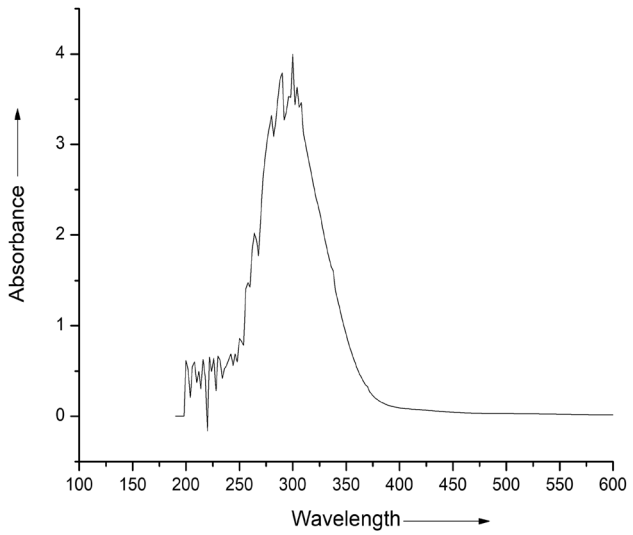

Fig. 2 UV–Vis Spectra of reaction product

spectra were recorded on JASCO FT-IR spectrometer using KBr pellets. UV–Vis spectra (Fig. 2) of above reaction were also documented which exhibited the outcomes in accordance with spectra.

Kinetic study of reaction orders

The order of reaction was calculated from the slope of log [conc.] vs. log dc/dt plots by varying the concentrations of MTZ, $HClO_4$, $KBrO_3$, Ru (III), and Hg $(OAc)_2$ in order such that rest of the concentrations and conditions were kept constant. The reaction was found to have the first-order dependence with respect to $KBrO_3$ between the concentration range of $\mathbf{1}.0\times10^{-3}$ to 2.25×10^{-3} mol dm^{-3} at fixed concentrations of MTZ, Ru^{III}, $HClO_4$, Hg $(OAc)_2$ (Figs. 3, 4, 5).

At a fixed Ru(III), $HClO_4$, $Hg(OAc)_2$ and $KBrO_3$, the apparent order in MTZ in the range 0.5×10^{-3} to 1.75×10^{-3} mol $dm^{-3}$was zero (Fig. 4). The effect of acid in the range of 0.1×10^{-3} to 3.0×10^{-3} mol dm^{-3} at fixed concentrations of Ru(III), MTZ, $KBrO_3$ and $Hg(OAc)_2$ at consistent ionic strength 0.005 mol dm^{-3} depicts that the rate constants dwindled with increase in alkali, i.e., negative order dependence on reaction rate. This was also confirmed by the linearity of the plots of log $[H^+]$ vs. log(dc/dt) ($r \geq -0.97839$, $S \leq 0.01639$) for different $[HClO_4]$ (Fig. 5). Addition of mercuric acetate at regular intervals shows that bromide ion had an inconsequential mark on the reaction rate [21]. This further corroborates that Hg

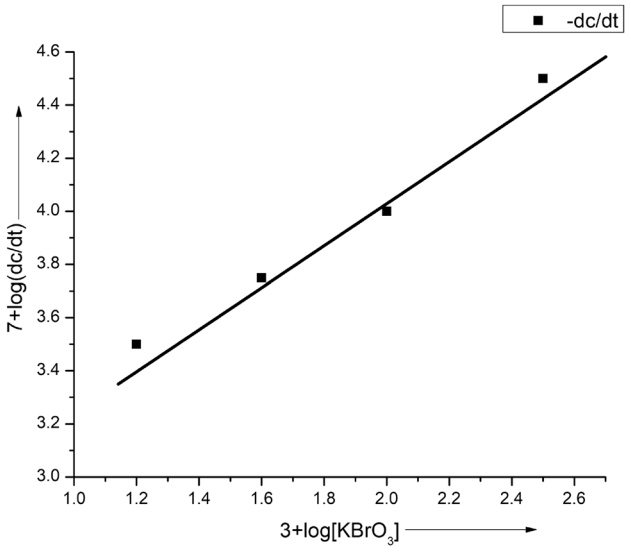

Fig. 3 Plot between rate of reaction $(-dc/dt)\times10^7$ vs $[KBrO_3\times10^{-3}]$ for the oxidation of MTZ at 35℃

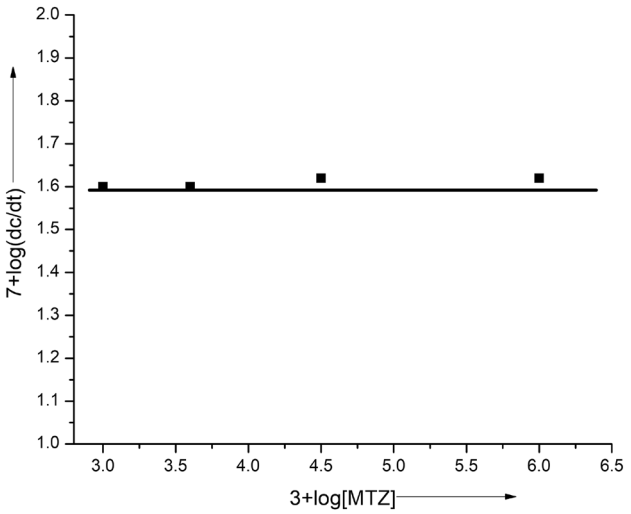

Fig. 4 Plot between rate of reaction (-dc/dt) × 10^7 vs [MTZ] × 10^{-3} on the reaction rate at 35℃

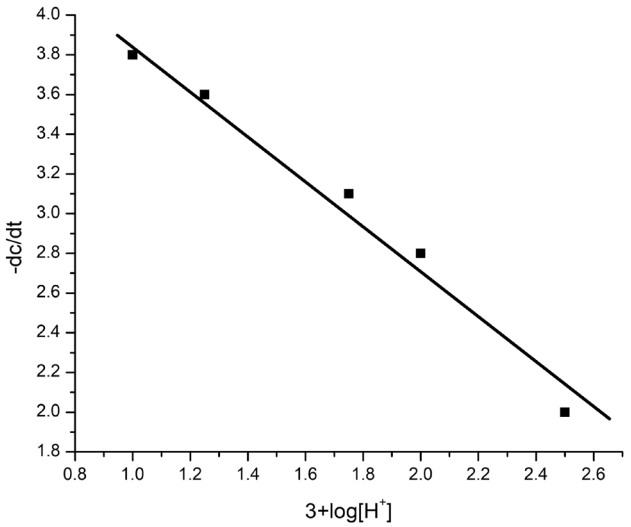

Fig. 5 Plot between rate of reaction (-dc/dt) × 107 vs [HClO4] × 10^{-3} on the reaction rate at 35℃

$(OAc)_2$ merely does sequestration for bromide ion formed during the reaction [22] (Table 1).

Dielectric constant and ionic strength variation

$KClO_3$ was used to study the ionic strength at concentrations between 0.1 and 0.9 mol dm^{-3}, keeping concentrations of other reactants constant at 30 °C. Likewise, the dielectric constant varied using acetic acid and water in different ratios [23]. Conclusively, both showed no appreciable effects on reaction rate [22, 24].

Effect of change of temperature-

The influence of the temperature on Ruthenium (III) catalyzed oxidation was studied at a temperature range between 30℃-45℃. Rate constants of the slowest step of the aforesaid Scheme were calculated through the intercepts and slopes of [Ru (III)]/k_1 vs. 1/[MTZ] at least four varying temperatures. Apparently, observations showed that the oxidation of MTZ was accelerated by augmenting the temperature.

Effect of change in concentration of catalyst –

The above reaction rate showed first-order dependence on [catalyst] in the 8.0×10^{-5}–8.0×10^{-4} mol dm^{-3} range. Reaction rate in the devoid of catalyst, under the given concentration conditions, was very incremental (Fig. 6). Order in Ru(III) was unity as confirmed by least square method and linearity of plots of log k_c versus log[Ru(III)] ($r \geq 0.9772$, $S \leq 0.04544$).

The electronic spectrum of the Ruthenium(III) solution employed is similar to that reported [25, 26] for the $[Ru(H_2O)_6]^{3+}$ spectrum [27]. Therefore, $[Ru(H_2O)_6]^{3+}$ is considered to be the most active species of Ru(III) under our experimental conditions [25, 26, 28].

Utility of scavenger

It is to be noted that reaction is assumed to be disencumbered by any free radical. This can be inferred by the negligible effect of mercuric acetate (Fig. 7).

It averts any parallel oxidation of bromine that the bromate and bromide ion interaction could have devised. The reported empirical rate constants, therefore, stand for pure bromate oxidation as Hg $(OAc)_2$ acts as a scavenger for any bromide ion formed (Fig. 7).

The presence of mercuric acetate (in excess of bromate concentration) clearly indicates that Br_2 oxidation has been completely subdued [29, 30]. Br_2 otherwise could have been formed by the interaction of Bromide ion and bromate as follows:

$$BrO_3^- + Br^- + 6H^- \rightarrow Br_2 + 3H_2O$$

Computational details of Ru (III) catalyzed oxidation of MTZ by Potassium Bromate in acidic medium-

Crystal structure and molecular geometry

The computational calculated longest distance of MTZ lies between C6–C7 is established to be 1.5295 Å, analogous to the experimental value (1.54 Å) which was a pure single bond character. Due to electron withdrawing group NO_2, the

Table 1 Effect of variation of [$KBrO_3$], [MTZ], [$HClO_4$], and [Ru(III)] on the Ruthenium (III) catalyzed oxidation of MTZ by $KBrO_3$in aqueous acidic medium at 298 K

$[KBrO_3]\times10^{-3}$ (mol dm^{-3})	$[MTZ]\times10^{-3}$ (mol dm^{-3})	$Ru(III)\times10^{-3}$ (mol dm^{-3})	$[HClO_4]\times10^{-3}$ (mol dm^{-3})	$[Hg(OAc)_2]\times10^{-4}$ (mol dm^{-3})	$(-dc/dt)\times10^{7}$ (mol dm^{-3} s^{-1})	$K_1\times10^{4}$ (Observed)
1.00	1.00	2.5	2.50	4.00	4.30	1.59
1.25	1.00	2.5	2.50	4.00	4.00	1.70
1.50	1.00	2.5	2.50	4.00	3.80	3.62
1.75	1.00	2.5	2.50	4.00	3.30	2.54
2.00	1.00	2.5	2.50	4.00	2.70	2.16
2.25	1.00	2.5	2.50	4.00	2.00	2.00
3.00	0.50	2.5	2.50	4.00	4.33	6.19
3.00	0.75	2.5	2.50	4.00	1.93	2.30
3.00	1.00	2.5	2.50	4.00	1.90	2.38
3.00	1.25	2.5	2.50	4.00	3.33	2.12
3.00	1.50	2.5	2.50	4.00	1.50	2.50
3.00	1.75	2.5	2.50	4.00	1.44	2.67
3.00	1.00	2.00	2.50	4.00	6.00	5.08
3.00	1.00	1.67	2.50	4.00	6.28	6.28
3.00	1.00	1.43	2.50	4.00	6.80	8.00
3.00	1.00	1.25	2.50	4.00	7.50	10.00
3.00	1.00	1.11	2.50	4.00	7.89	12.52
3.00	1.00	0.91	2.50	4.00	9.10	14.92
3.00	1.00	2.5	5.00	4.00	3.87	3.49
3.00	1.00	2.5	2.50	4.00	3.70	3.85
3.00	1.00	2.5	2.00	4.00	3.49	3.75
3.00	1.00	2.5	1.67	4.00	3.20	3.64
3.00	1.00	2.5	1.43	4.00	3.10	3.69
3.00	1.00	2.5	1.25	4.00	2.81	3.51
3.00	1.00	2.5	2.50	3.33	2.05	2.05
3.00	1.00	2.5	2.50	2.86	2.50	2.58
3.00	1.00	2.5	2.50	2.50	2.51	2.67
3.00	1.00	2.5	2.50	2.22	2.52	2.93
3.00	1.00	2.5	2.50	2.00	2.50	2.38
3.00	1.00	2.5	2.50	1.82	2.56	1.90

bond length between C2-H5 becomes shortest one. All C = C and C–H bond distances of rings are in the range 1.37– 1.52 and 1.07–1.09 Å, respectively. The symmetry of the ring, with an electron withdrawing nitro group, is distorted in ring angles at the point of substitution. In substituted imidazole ring there is a deviation in bond angle C1-N4-C3 since it decrease from 105.274° to 105.192° which may be attributed to the oxidation of alcoholic group to aldehydic carbonyl group at C7 (Fig. 8).

Product was obtained as needle shaped crystal by slow evaporation of solvent at room temperature and crystallized in triclinic system with space group C_1.In 2- (2-methyl-5-nitroimidazol-1-yl) acetaldehyde the computational calculated longest distance between C–C is 1.52 Å, analogous to the experimental value (1.54 Å) and this was exactly similar for all C–C bonds and the smallest bond lengths are in between C–H i.e., 1.08 almost similar to experimental value (1.09).

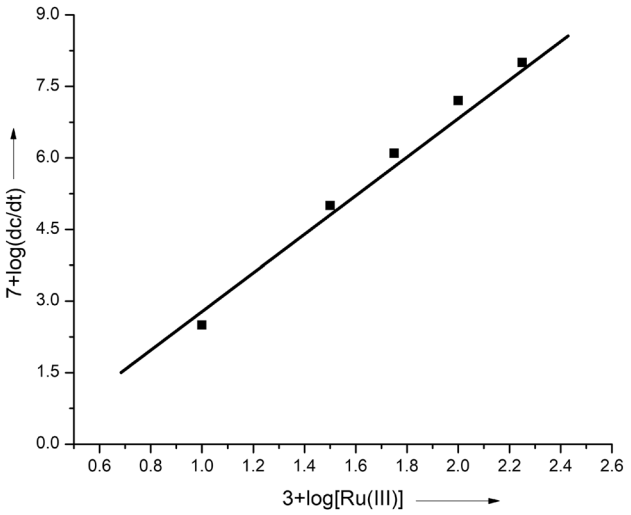

Fig. 6 Plot between rate of reaction $(-dc/dt)\times10^{7}$ vs $[Ru(III)]\times10^{-3}$ on the reaction rate at 35℃

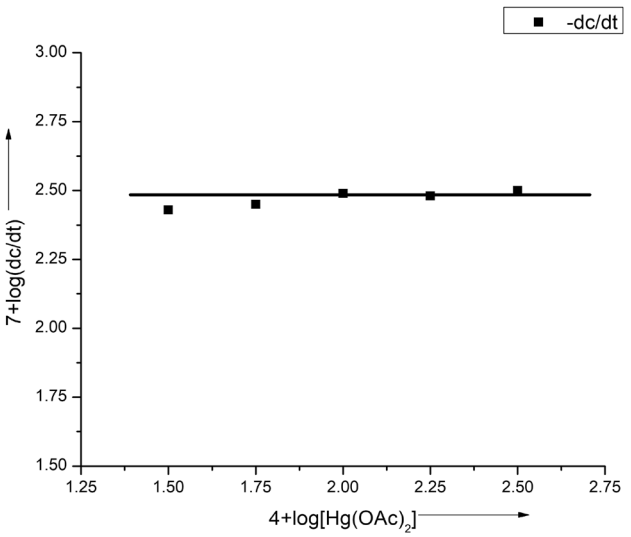

Fig. 7 Plot between rate of reaction $(-dc/dt)\times10^{7}$ vs $[Hg(OAc)_2]\times10^{-4}$ on the reaction rate at 35℃

Electronic absorption spectra

Formation of 2- (2-methyl-5-nitroimidazol-1-yl) ethanol as oxidation product of of metronidazole was ascertained by peak around 290 nm in UV–Vis Double-Beam Spectrophotometer (systronic-2203) instrument with water as a solvent (Fig. 2). The UV–Vis spectrum of reactant and compound have been studied by TD-DFT method using B3LYP an 6–31- (,p) basis sets. The solvent effect has been calculated using integral equation formalism polarizable continuum model (IEFPCM) [31, 32]. The UV data with oscillator strength (f), excitation energies, percentage contribution of anticipated transitions and resultant absorption wavelengths have been probed with experimental results. The theoretical UV spectrum of MTZ ($f=0.2359$) in water has a broad and intense electronic transition at 299 nm and product ($f=0.0042$) has electronic transition at 292 nm and, which complies with the measured experimental data of MTZ (303 nm in water) and Product (300 nm in water) (Fig. 2). The HOMO–LUMO of any molecule helps to explain the reactivity and kinetic sustainability of its interaction. If energy gap is less, then the compound is less stable since it favors the promotion of e– to less energy LUMO. The molecular orbital diagram shows that product has lowest HOMO–LUMO gap so it is more reactive than reactant (Fig. 9). The Vibrational theoretical spectra of the reactant and product show intense troughs at 1562 cm^{-1} and 1813 cm^{-1} which very well correlates with the experimental values at 1550 cm^{-1} and 1809 cm^{-1} (Fig. 1).

Molecular electrostatic potential

The molecular electrostatic potential (MESP) renders the electronic density and gives content about electrophilic, nucleophilic attack as well as hydrogen– bonding interactions [33]. Molecular electrostatic potential counter map are prepared by B3LYP/6- 31G(d,p) method using Gauss view 9.0 program. The molecular electrostatic potential contour surface of product and reactant is generated. The 3D surface MESP shows the negative regions are electrophilic regions,

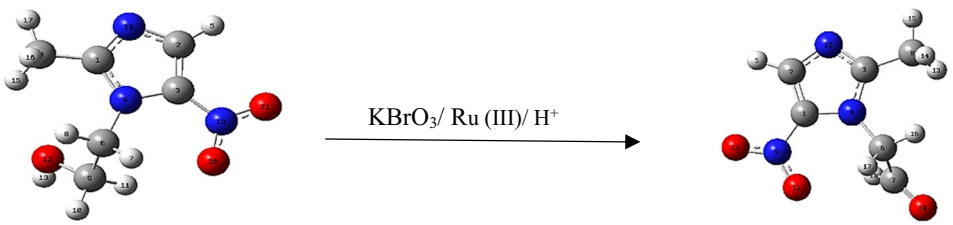

Metronidazole *2-(2-methyl-5-nitroimidazol-1-yl) ethanal*

Fig. 8 Optimized Structure of reactant and products

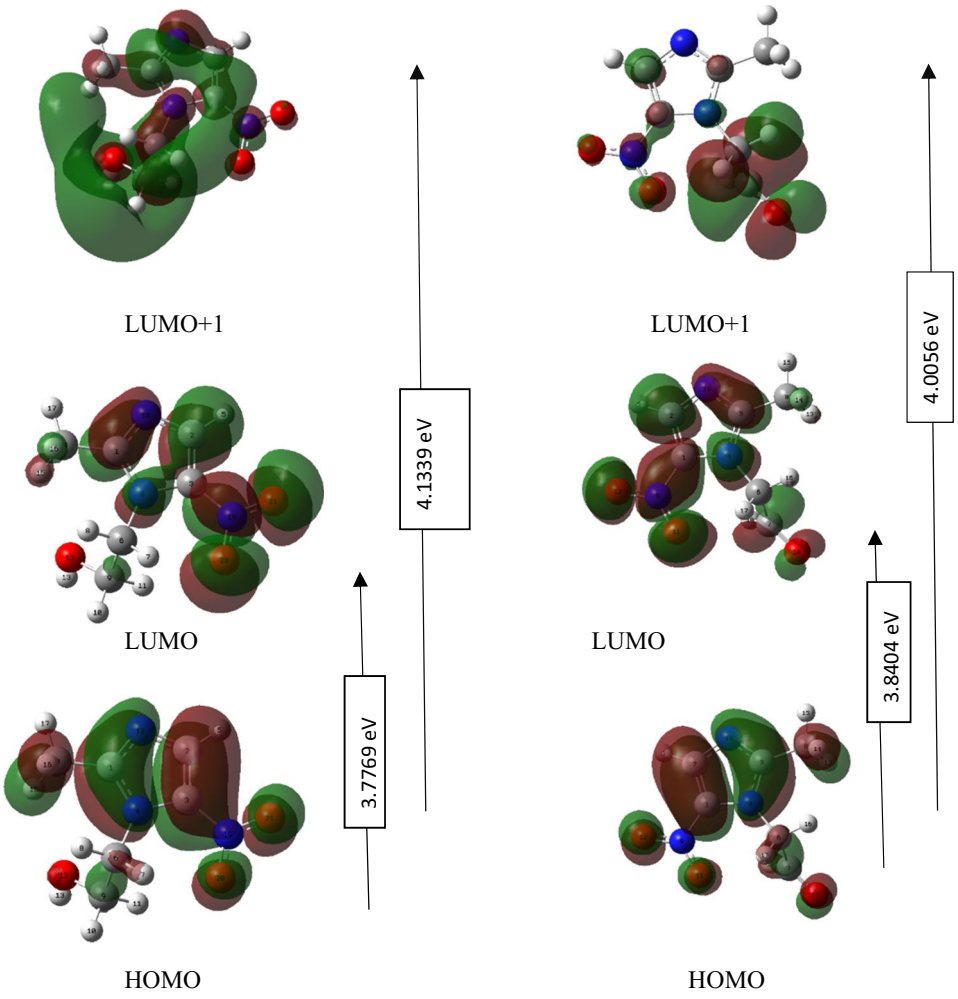

Fig. 9 HOMO–LUMO transitions for MTZ and main product

these are mainly over the oxygen and nitrogen atoms in reactant and in product, the positive regions are the nucleophilic regions and these are over the carbon atoms connected with oxygen and nitrogen atom and over the hydrogen atoms of the title molecule (Fig. 10). The MEP value of MTZ around O19 is + 7.443 and MEP values of Product around O19 are –9.49 and + 9.498, respectively. The red regions on oxygen atom assayed nucleophilic nature so it participate further in reaction with electrophilic while blue regions on hydrogen implies its electrophilic nature which can easily be abstracted by nucleophile [34].

Non-linear optical analysis

The utilization of NLO in telecommunication, broadcasting and optical interconnection is the current prevalent area for researchers. The dipole moment of product is 4.69 D which is much higher than MTZ while the calculated polarizability and hyper polarizability of product are 11.24×10^{-24} and 311.52×10^{-30} esu, respectively, that are higher than that of MTZ. Thus, product has more optical properties than reactant. The values for both reactant and product were found to be greater than those of urea ($\beta_{urea} = 0.3728 \times 10.^{-30}$ esu). Thus, both are good NLO material (Table 2).

$$\mu_{total} = \left(\mu_x^2 + \mu_y^2 + \mu_z^2\right)^{1/2},$$

$$\alpha_{total} = \frac{1}{3}\left(\alpha_{xx} + \alpha_{yy} + \alpha_{zz}\right),$$

$$\beta_{total} = \left[\left(\beta_{xxx} + \beta_{xyy} + \beta_{xzz}\right)^2 + \left(\beta_{yyy} + \beta_{xzz} + \beta_{yxx}\right)^2 + \left(\beta_{zzz} + \beta_{zxx} + \beta_{zyy}\right)^2\right]^{1/2}$$

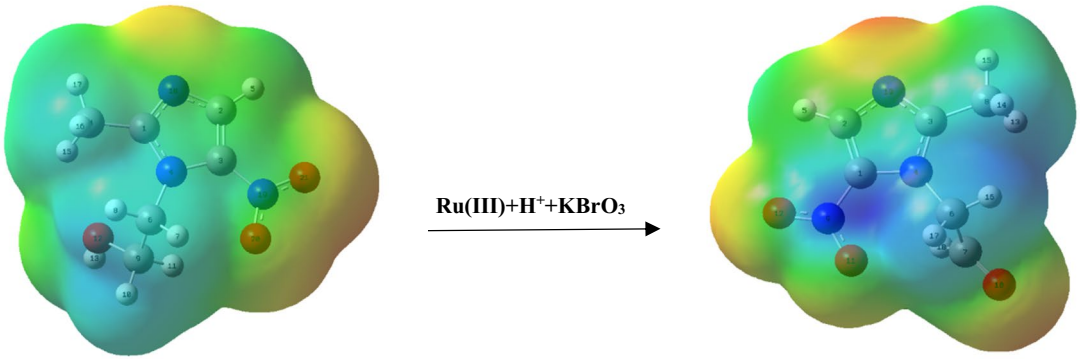

Fig. 10 3D plots of the molecular electrostatic potential of metronidazole and oxidation product

Table 2 NLO ANALYSIS

Dipole moment (μ_{tot}) (Debye)	B3LYP/6–31 + G(d,p)
μ_x	3.0159
μ_y	3.4747
μ_z	0.9214
μ_{tot}	4.6924
Polarizability	Values
α_{xx}	−76.7137
α_{xy}	+ 4.7816
α_{yy}	−84.4902
α_{xz}	+ 2.5364
α_{yz}	+ 0.8515
α_{zz}	−66.4987
$<\alpha>(esu)\times10^{-24}$	−11.24850844

Table 3 Global Reactivity Descriptors and Thermodynamic Analysis of the product

Parameter	Values
E_{HOMO}(eV)	− 7.598
E_{LUMO}(eV)	− 3.115
Ionization potential	7.598
Electron affinity	3.115
Energy gap(eV)	4.483
Electronegativity	5.356
Chemical potential	5.356
Chemical hardness	2.241
Chemical softness	0.446
Electrophilicity index	6.400

Global reactivity descriptors-

The DFT based Global reactivity descriptors are utilized for various aspects of chemical bonding, mechanism and reactive centers. Ionization potential (IP), electron affinity (EA), electronegativity (χ), chemical potential (μ), global hardness (η), global softness (S), and electrophilicity index (ω) [34] were calculated (Table 3).

$$IP = -\varepsilon_{HOMO},\ EA = -\varepsilon_{LUMO},$$

$$\chi = -\frac{1}{2}\left(\varepsilon_{HOMO} + \varepsilon_{LUMO}\right),\ \eta = -\frac{1}{2}(I - A)$$

$$\mu = -\frac{1}{2}(I + A),\ \omega = \frac{\mu^2}{2\eta},$$

$$S = \frac{1}{2\eta},\ \Delta N_{\max} = -\frac{\mu}{\eta}$$

As the HOMO–LUMO energy gap increases, the molecule becomes harder, which resist deformation of electron cloud. Higher the value of the electrophilicity index (ω) better is electrophilic character. Hence, reactant is less electrophilic than product which has electrophilicity index (ω) of 6.400.

Thermodynamic analysis Due to various chemical and physical phenomena thermodynamic analysis play consequential role. In present analysis, we have calculated various thermodynamic parameters such as chemical potential, electronegativity, ionization potential, etc. using DFT B3LYP/6-31G (d,p) method (Table 3). All the thermodynamic calculations are conducted in gas phase and not in solution (**Scheme**).

Discussion

Scheme

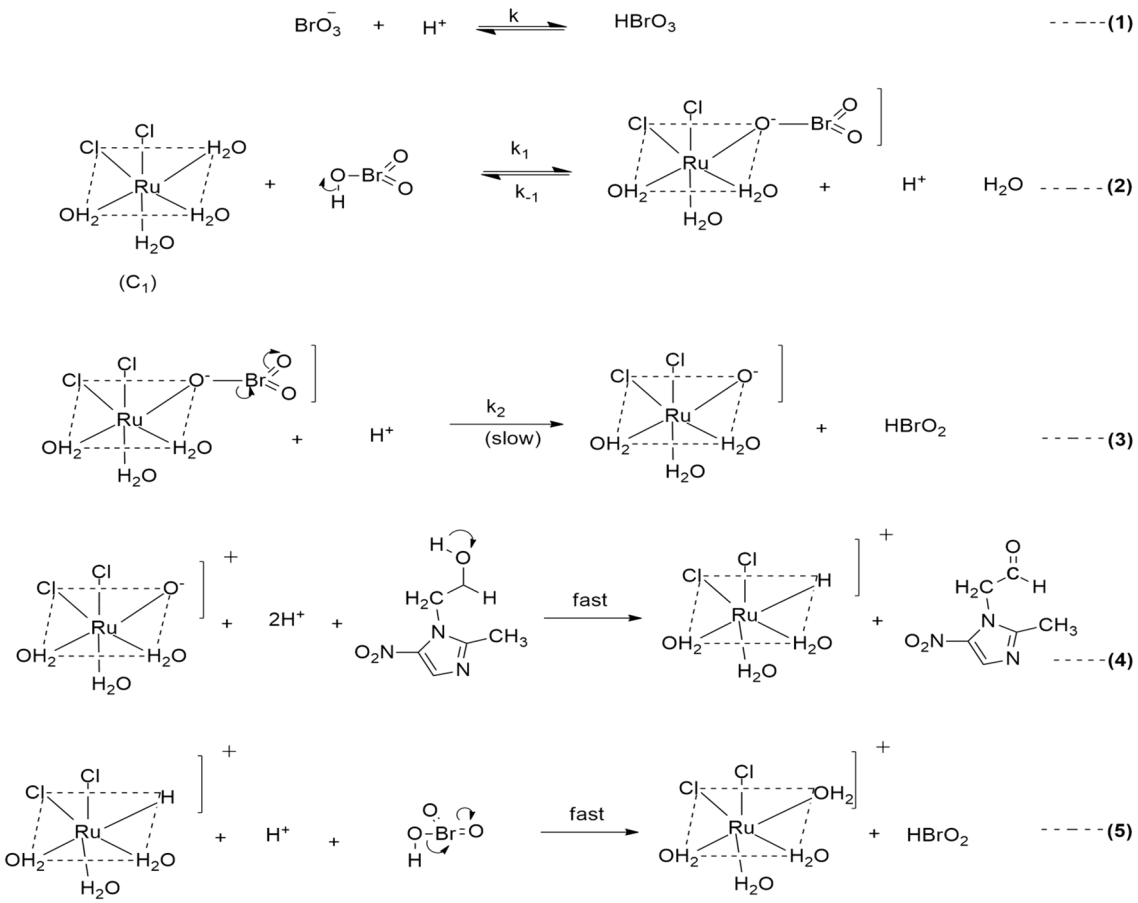

In the absence of catalyst oxidation of MTZ is very sluggish but it becomes facile in presence of Ru (III) catalyst. The observed modest enthalpy of activation and a higher rate constant for slow step indicates that oxidation presumably occurs via an inner-sphere mechanism. Reactive species of oxidant-catalyst, product and activation parameters have been identified. The observed results have been explained by mechanism and related law has been deduced.

The reaction follows 1:1 stoichiometry between bromate and MTZ in the presence of a ruthenium (III) as a catalyst. Orders were found to be unity in bromate and ruthenium (III) each, but zeroth order in substrate and negative fractional order in $[H^+]$.

Based on the above discussions and observed kinetic data, a potential mechanism is offered for the oxidation of MTZ (**Scheme**).

Rate law

$$\frac{-d[BrO_3^-]}{dt} = k_2\,[C_2]\,[H^+] \quad (1)$$

$$\frac{d[C_2]}{dt} = k_1\,[C_1]\,[HBrO_3] - k_{-1}\,[C_2]\,[H^+] - k_2\,[C_2]\,[H^+] \quad (2)$$

$$\text{at steady state, } \frac{d[C_2]}{dt} = 0 \quad (3)$$

From (2) and (3) we have;

$$k_1\,[C_1]\,[HBrO_3] = [C_2]\,[H^+]\,\{k_{-1} + k_2\}$$

or

$$[C_2] = \frac{k_1\,[C_1][HBrO_3]}{[H^+]\,\{k_{-1}+k_2\}} \quad (4)$$

$$k_1\,[C_1][HBrO_3] = [C_2][H^+]\{k_{-1} + k_2\}$$
or
$$[C_2] = \frac{k_1\,[C_1][HBrO_3]}{[H^+]\{k_{-1}+k_2\}} \quad (5)$$

From (1),

$$\frac{-d[BrO_3^-]}{dt} = \frac{k_2 k_1 [H^+]\,[C_1][HBrO_3]}{[H^+]\{k_{-1}+k_2\}}$$
or,

$$\frac{-d[BrO_3^-]}{dt} = k_2\,\frac{k_1[C_1][HBrO_3]}{\{k_{-1}+k_2\}} \quad (6)$$
$$[Ru^{III}] = [C_1] + [C_2]$$

By (4) and (6);

$$[Ru^{III}] = [C_1] + \frac{k_1\,[C_1][HBrO_3]}{[H^+]\{k_{-1}+k_2\}}$$
$$[Ru^{III}] = [C_1]\left\{1 + \frac{k_1\,[HBrO_3]}{[H^+]\{k_{-1}+k_2\}}\right\}$$
$$[Ru^{III}] = [C_1]\left\{1 + \frac{[H^+](k_{-1}+k_2)+k_1[HBrO_3]}{[H^+](k_{-1}+k_2)}\right\} \quad (7)$$
$$[C_1] = \frac{[H^+](k_{-1}+k_2)[Ru^{III}]}{[H^+](k_{-1}+k_2)+k_1\,[HBrO_3]}$$

From (5);

$$\frac{-d[BrO_3^-]}{dt} = \frac{k_1k_2[HBrO_3]}{\{k_{-1}+k_2\}}\,\frac{[H^+](k_{-1}+k_2)[Ru^{III}]}{[H^+](k_{-1}+k_2)+k_1\,[HBrO_3]}$$
or, (8)
$$\frac{-d[BrO_3^-]}{dt} = \frac{k_1k_2[Ru^{III}][H^+][HBrO_3]}{[H^+](k_{-1}+k_2)+k_1[HBrO_3]}$$

If $k_1\,k_2$ and k_2 can be neglected;

$$\frac{-d[BrO_3^-]}{dt} = \frac{k_1k_2[Ru^{III}][H^+][HBrO_3]}{k_{-1}[H^+]+k_1[HBrO_3]} \quad (9)$$

Also $k_{-1}\,[H+]\,k_1\,[HBRO_3]$

$$\text{and } [HBrO_3] = [BrO_3^-] \text{ at constant } [H^+] \quad (10)$$

Therefore Eq. (9) becomes,

$$\frac{-d[BrO_3^-]}{dt} = k_1k_2[Ru^{III}][BrO_3^-] \quad (11)$$

Therefore, the rate law (11) conforms well to the experimental observations.

Conclusions

The kinetics of oxidation of Metronidazole by Potassium Bromate with Ru(III)[35] as catalyst in acidic medium follows first-order kinetics with respect to oxidant and catalyst and zero order with respect to substrate. The above reaction rates are obtained experimentally and corroborates well with that of available theoretical. The rate law is in adherence with all kinetic observations and propound mechanistic steps are supported by the trifling effect of ionic strength. Uniform effect of acetic acid addition signifies a footling dielectric effect. From these investigations, it is concluded that BrO_3^- [13] and $[Ru(H_2O)_6]^{3+}$ are the reactive species of $KBrO_3$ and $RuCl_3$, respectively, in acidic medium. The observed results were explained by plausible mechanisms and the related rate laws were deduced which were further justified by the application of computational approach. Since the HOMO–LUMO energy gap of product is lower than MTZ so oxidation product is more stable. On basis of NLO calculations value of βo for both reactant and product were higher than urea so both have good optical property. There is, thus, urgent need to find alternative ways by which the biological toxicity of this particular drug can be dealt in a productive manner. Such oxidative study of MTZ interpret the mechanism of transfiguration of such compounds in biological systems which is of utmost biological and industrial significance. [36].

Acknowledgements The authors convey their profound thanks to the Head, Department of Chemistry, Lucknow University for providing laboratory facilities for spectral analysis and central facility for computational research.

Funding This research received no external funding.

Declarations

Conflict of interest No conflict of interest is reported by the authors.

References

1. B. Rafique, K. Shafique, S. Hamid, S. Kalsoom, M. Hashim, B. Mirza, L. Jafri, M. Iqbal, J. Biomol. Struct. Dyn. **40**(12), 5446–5461 (2022)
2. R.V. Jagadeesh, N.M. Made, Gowda., Oxidation of metronidazole with sodium N-bromo-p-toluenesulfonamide in acid and alkaline media: a kinetic and mechanistic study. Int. J. Chem. Kinetics **37**(11), 700–709 (2005). https://doi.org/10.1002/kin.20118
3. K.N. Mohana, P.M. Ramdas Bhandarkar, Mechanistic investigation of oxidation of metronidazole and tinidazole with N-bromosuccinimide in acid medium: a kinetic approach. J. Iran. Chem. Soc. **6**(2), 277–287 (2009)
4. N.A. Farook, Kinetics and mechanism of oxidation of 4-oxoacids by N-bromosuccinimide in aqueous acetic acid medium. J. Iran. Chem. Soc. **3**(4), 378–386 (2006)
5. S.M. Desai, N.N. Halligudi, S.T. Nandibewoor, Kinetics and mechanism of ruthenium(III)-catalysed oxidation of allyl alcohol by acid bromate-autocatalysis in catalysis. Trans. Metal Chem. **27**, 207–212 (2002)
6. H.A. Young, The reduction of bromic acid by hydrobromic acid in the presence of hydrogen peroxide. J. Am. Chem. Soc. **72**(7), 3310–3312 (1950)
7. V. Avasthi, A.C. Chatterji, Mechanism of Oxidation of Simple Organic Molecules Part XX. Z. Phys. Chem. **245**(1), 154–160 (1970)

8. R. Natarajan, W. Venkatasubramanian, The kinetics of oxidation of secondary alcohols by potassium bromate. Tetrahedron Lett. **10**(57), 5021–5024 (1969)
9. S. Reddy, Cherkupally, and Tumu Vijaya Kumar., Aquachlororuthenium (III) complex catalysis in the oxidation of malonic and methylmalonic acids by bromate in perchloric acid medium Study of induction period and evaluation of individual kinetic parameters. Transition Met. Chem. **32**(2), 246–256 (2007)
10. Murthy, N. Krishna, Ch Sanjeeva Reddy, and E. V. Sundaram. (1989). Kinetics & Mechanism of Acid Bromate Oxidation of Aliphatic, Aralkyl & Alicyclic Ketones.
11. S.B. Jonnalagadda, R.H. Simoyi, G.K. Muthakia, A kinetic study of the oxidation of indigo carmine with acidic bromate. J. Chem. Soc. Perkin Trans. **7**, 1111–1115 (1988)
12. C.M. Santana, Z.S. Ferrera, M.E.T. Padron, J.J.S. Rodrıguez, Analytical methodologies for the determination of nitroimidazole residues in biological and environmental liquid samples: a review. Anal Chim Acta **665**, 113–122 (2010)
13. B. Singh, A. Ratan, V. Prakash, D. Mala Kesarwani, A kinetic and mechanistic study of Ru (III) catalysis in acid bromate oxidation of butyl diethylene glycol. Oxidation Commun. **19**, 552–558 (1996)
14. A.I. Vogel, Text Book of Quantitative Chemical Analysis, 5th edit., ELBS, Longman, 407(1989).
15. Y.C. Houricichi and I. Osamu, Chem. Abstr., 72, 50,624 (1970); D.L. Kamble, R.B. Chougale and S.T. Nandibewoor, Indian J. Chem., 35A, 865 (1996).
16. A. Srivastava, M. Gupta, S. Srivastava, Kinetic, spectroscopic, and DFT studies of novel oxidation of acetylsalicylic acid by NaIO4 using micro-amount of Os (VIII) as a homogeneous catalyst in alkaline medium. Russ. J. Phys. Chem. A **93**(10), 2023–2031 (2019). https://doi.org/10.1134/S0036024419100297
17. E.D. Glendening, J.K. Badenhoop, A.E. Reed, J.E. Carpenter, J.A. Bohmann, C.M. Morales, F. Weinhold, *NBO, version 5.0* (Theoretical Chemistry Institute, University of Wisconsin, Madison, WI, 2001)
18. M. Cossi, V. Barone, Time-dependent density functional theory for molecules in liquid solutions. J. Chem. Phys. **115**(10), 4708–4717 (2001)
19. D.S. Mahadevappa, H.M.K. Naidu, Talanta **20**, 349 (1973)
20. F. Feigl, V. Anger, *Spot Tests in Organic Analysis*, vol. 416 (Elsevier, London, 1975)
21. J.C. Bailar, The Chemistry of Coordination Compounds, Reinhold: New York, 1966, p. 4; N. Venkatasubramanian and V. Thiagarajan, Can. J. Chem., 47, 694 (1969); E. Koros, M. Varga and L. Gyorgyi, J. Phys. Chem., 88, 4116 (1984); C.S. Reddy and T. Vijayakumar, Indian J. Chem., 34A, 615 (1995)
22. E. W. Washburn, Ed., (1932) International Critical Tables of Numerical Data Physics Chemistry and Technology McGraw-Hill, New York, G. Akerloff, J. Am. Chem. Soc., 54, 4125
23. C.K. Ingold, *Structure and Mechanism in Organic Chemistry*, 2nd edn. (G. Bell and Sons, London, 1969)
24. R. Venkata Nadh, B. Syama Sundar, P.S. Radhakrishnamurti, Kinetics of ruthenium (III) catalyzed and uncatalyzed oxidation of monoethanolamine by N-bromosuccinimide. Russian Journal of Physical Chem. A **90**(9), 1760–1765 (2016)
25. C.S. Reddy and T.V. Kumar, Indian J. Chem., 34A, 871 (1995); ibid, Indian J. Chem., 36A, 57 (1997).
26. F.A. Cotton and G. Wilkinson, Advanced Inorganic Chemistry, 5th edit., Wiley Interscience, New York, 1988, p. 885; D. Connick and D.A. Fine, J. Am. Chem. Soc., 83, 3414 (1961); 82, 4187 (1960).
27. B. Sethuram, *Some Aspects of Electron Transfer Reactions Involving Organic Molecules, Allied Publishers (P) Ltd* (Mumbai, India, 2003)
28. P.N. Naik, M. Prathiksha, S.K. Mahesh, B.J. Gayatri, M.K. Bhavani, V.P. Roopa, G.S. Anita, S.A. Chimatadar, S.T. Nandibewoor, Oxidative transformation of metronidazole by alkaline permanganate: kinetic and mechanistic study. International Journal of Drug Formulation and Research **4**(1), 36–53 (2013)
29. Srivastava, Amrita, Madhu Gupta, and Sheila Srivastava. "Os (VIII) Catalyzed Oxidative Cleavage of Pyrrolidine Ring in L-Proline by Sodium Periodate ($NaIO_4$) in Alkaline Medium." (2017).
30. H.H. Cady, R.E. Conick, J. Am. Chem. Soc. **80**, 2646 (1958)
31. C. Adamo, V. Barone, A TDDFT study of the electronic spectrum of s-tetrazine in the gas-phase and in aqueous solution. Chem. Phys. Lett. **330**(1–2), 152–160 (2000)
32. N. Prabavathi, N. Senthil Nayaki, The spectroscopic (FT-IR, FT-Raman and NMR), first order hyperpolarizability and HOMO–LUMO analysis of 2-mercapto-4 (3H)-quinazolinone. Spectrochim. Acta Part A Mol. Biomol. Spectrosc. **129**, 572–583 (2014)
33. S.K. Saha, A. Hens, N.C. Murmu, P. Banerjee, A comparative density functional theory and molecular dynamics simulation studies of the corrosion inhibitory action of two novel N-heterocyclic organic compounds along with a few others over steel surface. J. Mol. Liq. **215**, 486–495 (2016)
34. R.G. Parr, L.V. Szentpály, S. Liu, Electrophilicity index. J. Am. Chem. Soc. **121**(9), 1922–1924 (1999)
35. R. Natarajan, N. Venkatasubramanian, Kinetics and mechanism of oxidation of secondary alcohols by potassium bromate. Tetrahedron **30**(16), 2785–2789 (1974)
36. C.V. Hiremath, T.S. Kiran, S.T. Nandibewoor, Os(VIII)/Ru(III) catalyzed oxidation of aspirin drug by a new oxidant, Diperiodatoargentate(III) in aqueous alkaline medium: A comparative kinetic study. J. Mol. Catal. A. **248**, 163–174 (2006)